

Supplementary Information

Efficient photoswitchable organometallic complexes with azobenzene and stilbene units: the case of Au(I)

Stanislav Petrovskii,^a Anna Senchukova,^a Vladimir Sizov,^a Aleksandra Paderina,^a Maksim Luginin,^a Evgenia Abramova,^a and Elena Grachova^{a}*

^a *Institute of Chemistry, St Petersburg University, 198504 St. Petersburg, Russia*

Correspondence e.grachova@spbu.ru

Content

X-ray structure determinations of Au(I) complexes 1N–6N	4
Table S1. Crystallographic data for compounds 1N–6N	5
Table S2. Selected structural parameters for compounds 1N–3N	6
Table S3. Selected structural parameters for compounds 4N–6N	6
Table S4. Optical properties of LC , LN and Au(I) complexes XN (X = 1–6), XC (X = 1, 5, 6), DCE, c = 10 ⁻⁵ M, r.t.....	7
Table S5. Photoisomerization quantum yields of LC , LN and Au(I) complexes XN (X = 1–6), XC (X = 1, 5, 6), DCE, c = 10 ⁻⁵ M, r.t.; AB = native azobenzene.....	7
Table S6. Brief summary of the most important singlet excited states of XN and XC compounds as obtained from TDDFT calculations.....	8
Figure S1. ¹ H NMR spectra of 1N–3N , Acetone- <i>d</i> ₆ , r.t.....	9
Figure S2. ¹ H NMR spectra of 4N and 5N , Chloroform- <i>d</i> , r.t.....	10
Figure S3. ¹ H NMR spectrum of 6N , Acetone- <i>d</i> ₆ , r.t.	10
Figure S4. ¹ H NMR spectrum of 1C , Acetone- <i>d</i> ₆ , r.t.	11
Figure S5. ¹ H NMR spectrum of 5C , Chloroform- <i>d</i> , r.t.	11
Figure S6. ¹ H NMR spectrum of 6C , Chloroform- <i>d</i> , r.t.	12
Figure S7. FTIR spectra of azobenzene and stilbene derivatives, KBr pellet, r.t	12
Figure S8. Experimental ESI ⁻ MS spectra of 6N and 6C , and simulated isotopic patterns of the most intensive signal corresponded to molecular ion.....	13
Figure S9. Molecular structure of 2N , 3N and 5N	14
Figure S10. Mutual orientation of two molecules in the crystal packing of 3N	14
Figure S11. Mutual orientation of two molecules in the crystal packing of 4N	15
Figure S12. Mutual orientation of two molecules in the crystal packing of 5N	15
Figure S13. Mutual orientation of molecules in the crystal packing of 6N	15
Figure S14. UV-vis spectra of LN and Au(I) complexes XN (X = 1–3) before and after (line marked by ‘A’) UV irradiation, DCE, r.t. In the cases of irradiated samples formal ε values based on total concentrations are calculated.....	16

Figure S15. UV-vis spectra of Au(I) complexes XN ($X = 4–6$) before and after (line marked by ‘A’) UV irradiation, DCE, r.t. In the cases of irradiated samples formal ϵ values based on total concentrations are calculated.....	17
Figure S16. UV-vis spectra of LC and Au(I) complexes XC ($X = 1, 5, 6$) before and after (line marked by ‘A’) UV irradiation, DCE, r.t. In the cases of irradiated samples formal ϵ values based on total concentrations are calculated.....	18
Figure S18. Dihedral energy scans corresponding to rotation around N=N and C=C bonds: DFT computational data.....	22
Figure S19. Energy level diagram of the excited states in XN obtained from TDDFT calculations. Colour legend shows singlets (blue), triplets (green), and low-lying active states (red).	23
Figure S20. Energy level diagram of the excited states in XC obtained from TDDFT calculations. Colour legend shows singlets (blue), triplets (green), and low-lying active states (red).	24
Figure S21. Evolution of the S_1 state in LN upon low-angle rotation around the N=N bond. Wavelengths and oscillator strengths are obtained from TDDFT calculations. Ground state energy curve is shown to demonstrate the relatively high probabilities of such rotations via comparison with kT value at room temperature.	25
Figure S22. Natural transition orbitals involved in the lowest energy electronic excitation for compound LN	26
Figure S23. Natural transition orbitals involved in the lowest energy electronic excitation for compound LC	27
Figure S24. Natural transition orbitals involved in the lowest energy electronic excitation for compounds 5N and 6N in <i>trans</i> -form of switcher group.....	28
Figure S25. Natural transition orbitals involved in the lowest energy electronic excitation for compounds XC ($X = 1, 5, 6$) in <i>trans</i> -form of switcher group.	29
Figure S26. Natural transition orbitals involved in the lowest energy electronic excitation for compounds 1C and 6C in <i>cis</i> -form of switcher group.	30
Figure S27. Emission spectrum of xenon lamp in soft UV region.	31
References	31

X-ray structure determinations of Au(I) complexes **1N–6N**

The crystal structures of **1N–6N** were determined by the means of single crystal X-ray diffraction analysis. Crystals were fixed on a micro mounts and the diffraction data have been collected on the various Rigaku Oxford Diffraction diffractometers at a temperature of 100K. Crystals of **1N**, and **3N–5N** was placed on the XtaLAB Synergy-S diffractometer and measured using monochromated CuK α radiation. Crystals of **2N** and **6N** were placed on the Agilent Supernova diffractometer and measured using monochromated CuK α radiation. Data were integrated and corrected for background, Lorentz, and polarization effects. An empirical absorption correction based on spherical harmonics implemented in the SCALE3 ABSPACK algorithm was applied in *CrysAlisPro* program.¹ The unit-cell parameters were refined by the least-squares techniques. The structures were solved by dual-space algorithm and refined using the *SHELX* programs^{2,3} incorporated in the *OLEX2* program package.⁴ The final models included coordinates and anisotropic displacement parameters for all non-H atoms. The carbon-bound H atoms were placed in calculated positions and were included in the refinement in the ‘riding’ model approximation, U_{iso}(H) set to 1.5U_{eq}(C) and C–H 0.96 Å for the CH₃ groups, U_{iso}(H) set to 1.2U_{eq}(C) and C–H 0.97 Å for the CH₂ groups and U_{iso}(H) set to 1.2U_{eq}(C) and C–H 0.93 Å for the CH groups. Supplementary crystallographic data for this paper have been deposited at Cambridge Crystallographic Data Centre (CCDC 2162085 – 2162090) and can be obtained free of charge via www.ccdc.cam.ac.uk/structures/.

Table S1. Crystallographic data for compounds **1N–6N**

Compound	1N	2N	3N	4N	5N	6N
Formula	C ₃₅ H ₃₀ AuN ₂ O ₃ P	C ₃₂ H ₂₁ AuF ₃ N ₂ P	C ₃₂ H ₂₄ AuN ₂ P	C ₂₃ H ₂₅ AuN ₄	C ₂₇ H ₂₇ AuN ₄	C ₆₄ H ₄₈ AuN ₅ P ₂
Crystal system	triclinic	monoclinic	triclinic	monoclinic	triclinic	monoclinic
<i>a</i> (Å)	12.42947(17)	12.29040(10)	10.33940(10)	17.7163(5)	9.98990(10)	14.8468(2)
<i>b</i> (Å)	12.6315(2)	17.49240(10)	10.83140(10)	10.5957(3)	13.60260(10)	16.8602(2)
<i>c</i> (Å)	22.1433(4)	12.96260(10)	12.85120(10)	11.3229(2)	18.30690(10)	21.2660(4)
α (°)	73.6773(15)	90	70.5120(10)	90	90.6340(10)	90
β (°)	80.9946(13)	102.5220(10)	89.9380(10)	94.813(2)	96.8150(10)	105.031(2)
γ (°)	71.2088(14)	90	71.5480(10)	90	103.8920(10)	90
<i>V</i> (Å ³)	3150.26(10)	2720.52(4)	1278.19(2)	2118.00(9)	2395.85(3)	5141.17(14)
Molecular weight	754.54	718.44	664.47	554.43	604.49	1145.98
Space group	P-1	P2 ₁ /c	P-1	P2 ₁ /c	P-1	I2/a
μ (mm ⁻¹)	9.549	11.102	11.582	13.159	11.693	6.326
Temperature (K)	100(1)	100.01(10)	99.99(10)	100.00(10)	99.99(10)	100(2)
<i>Z</i>	4	4	2	4	4	4
<i>D</i> _{calc} (g/cm ³)	1.591	1.754	1.726	1.739	1.676	1.481
Crystal size (mm ³)	0.14 × 0.12 × 0.08	0.133 × 0.081 × 0.042	0.074 × 0.053 × 0.021	0.258 × 0.213 × 0.173	0.273 × 0.214 × 0.198	0.159 × 0.133 × 0.118
Diffractometer	XtaLAB Synergy, HyPix	SuperNova, HyPix3000	XtaLAB Synergy, HyPix	XtaLAB Synergy, HyPix	XtaLAB Synergy, HyPix	SuperNova, HyPix3000
Radiation	CuK α	CuK α	CuK α	CuK α	CuK α	CuK α
Total reflections	47674	33659	47793	37734	103493	23526
Unique reflections	13146	5187	5271	4461	10013	4675
Angle range 2θ (°)	4.168 – 160.47	7.368 – 140.998	7.348 – 154.286	5.006 – 154.89	4.866 – 155.056	6.782 – 136.67
Reflections with <i>F</i> _o ≥ 4σ _{<i>F</i>}	11390	4780	5113	4336	9504	4515
<i>R</i> _{int}	0.0695	0.0416	0.0991	0.0647	0.0489	0.0411
<i>R</i> _σ	0.0494	0.0254	0.0376	0.0310	0.0204	0.0249
<i>R</i> ₁ (<i>F</i> _o ≥ 4σ _{<i>F</i>})	0.0589	0.0293	0.0292	0.0341	0.0314	0.0254
w <i>R</i> ₂ (<i>F</i> _o ≥ 4σ _{<i>F</i>})	0.1416	0.0789	0.0680	0.0929	0.0706	0.0629
<i>R</i> ₁ (all data)	0.0678	0.0315	0.0300	0.0346	0.0328	0.0263
w <i>R</i> ₂ (all data)	0.1473	0.0806	0.0683	0.0936	0.0714	0.0633
S	1.048	1.087	1.039	1.104	1.096	1.123
ρ _{min} , ρ _{max} , e/Å ³	–1.46, 3.63	–1.12, 2.52	–1.45, 1.14	–2.53, 1.35	–3.64, 2.98	–1.18, 0.62
CCDC	2162085	2162086	2162087	2162088	2162089	2162090

$R_1 = \Sigma ||F_o| - |F_c|| / \Sigma |F_o|$; $wR_2 = \{\Sigma [w(F_o^2 - F_c^2)^2] / \Sigma [w(F_o^2)^2]\}^{1/2}$; $w = 1 / [\sigma^2(F_o^2) + (aP)^2 + bP]$, where $P = (F_o^2 + 2F_c^2)/3$; $s = \{\Sigma [w(F_o^2 - F_c^2)] / (n - p)\}^{1/2}$ where n is the number of reflections and p is the number of refinement parameters.

Table S2. Selected structural parameters for compounds **1N–3N**

	1N	2N	3N
Bond lengths and distances, Å			
Au1–P1	2.2737(16)	2.2697(8)	2.2762(10)
Au2–P2	2.2725(19)	—	—
Au1–C14	2.032(6)	2.007(3)	1.999(4)
Au2–C49	1.977(7)	—	—
C13–C14	1.171(11)	1.191(5)	1.201(6)
C48–C49	1.218(11)	—	—
Bond angles, °			
P1–Au1–C14	172.3(2)	177.93(10)	173.38(11)
P2–Au2–C49	173.0(2)	—	—
Au1–C14–C13	134.5(1)	175.4(3)	169.6(4)
Au2–C49–C48	176.3(6)	—	—

Table S3. Selected structural parameters for compounds **4N–6N**

	4N	5N	6N
Bond lengths and distances, Å			
Au1–C15	2.021(4)	2.036(4)	—
Au1A–C15A	—	2.022(5)	—
Au1–C14	1.989(4)	1.991(4)	2.004(3)
Au1A–C14A	—	1.985(5)	—
C13–C14	1.199(6)	1.192(6)	1.190(4)
C13A–C14A	—	1.200(7)	—
Bond angles, °			
C14–Au1–C15	178.42(14)	176.77(16)	—
C14A–Au1–C15A	—	178.25(18)	—
C14–Au1–C14'	—	—	179.28(15)
Au1–C14–C13	171.4(3)	172.6(4)	177.6(2)
Au1–C14A–C13A	—	174.7(4)	—

Table S4. Optical properties of **LC**, **LN** and Au(I) complexes **XN** (X = 1–6), **XC** (X = 1, 5, 6), DCE, c = 10⁻⁵ M, r.t.

Compound	λ_{abs} , nm (ϵ , 10 ⁴ cm ⁻¹ M ⁻¹)		Bathochromic shift*, cm ⁻¹
	Before irradiation	After UV irradiation	
LN	336(3.63)	437(0.25), 308 ^{sh} (0.88), 263(2.0)	—
1N	365(2.84), 255(5.15)	446(0.28), 334 ^{sh} (1.07), 255(5.15)	2365
2N	364(3.23)	448(0.29), 337 ^{sh} (1.09), 290(1.73)	2289
3N	364(3.01)	448(0.26), 338 ^{sh} (0.99), 291(1.55)	2289
4N	372(3.75), 279 ^{sh} (1.0), 257 ^{sh} (1.86)	450(0.33), 351(1.33), 283(1.82), 258(1.93)	2880
5N	369(3.53), 291(2.25), 283 ^{sh} (1.94)	452(0.32), 340(1.36), 292(2.98), 284(2.43)	2662
6N	397(6.44)	385(3.68), 465(0.72)	4573
LC	340 ^{sh} (1.89), 322(2.94), 310 ^{sh} (2.63)	339 ^{sh} (0.75), 322 ^{sh} (1.35), 311(1.50), 298 ^{sh} (1.41)	—
1C	358 ^{sh} (3.67), 340(5.29), 326 ^{sh} (4.31)	319(2.83)	1644**, 1479**
5C	358 ^{sh} (4.53), 341(6.28), 329 ^{sh} (5.10)	328 ^{sh} (2.22), 312(2.68)	1730**, 1479**
6C	367 (10.97), 351(10.55)	334 ^{sh} (2.64), 318(3.14)	2566**, 2164**

* compared to band of transition in azobenzene or stilbene moiety of free acetylenes **LN** or **LC** before irradiation, respectively

** calculated for two lowest maximums

Table S5. Photoisomerization quantum yields of **LC**, **LN** and Au(I) complexes **XN** (X = 1–6), **XC** (X = 1, 5, 6), DCE, c = 10⁻⁵ M, r.t.; **AB** = native azobenzene.

Sample	Light source, wavelength	Photon flux, photons/s	ϵ , cm ⁻¹ M ⁻¹		$\Phi_{\text{trans} \rightarrow \text{cis}}$
			<i>trans</i>	<i>cis</i>	
AB*	Laser, 355 nm	1.103369E+16	3860	449	0.11
LN	Laser, 355 nm	1.103369E+16	17020	1230	0.09
AB*	Xenon lamp, 355 nm	8.0422E+13	3860	449	0.11
LN	Xenon lamp, 355 nm	8.0422E+13	17020	1230	0.10
1N	Xenon lamp, 382 nm	2.983E+14	25070	6153	0.13
2N	Xenon lamp, 382 nm	2.983E+14	25520	4221	0.13
3N	Xenon lamp, 382 nm	2.983E+14	27510	4150	0.12
4N	Xenon lamp, 382 nm	2.983E+14	32096	9063	0.15
5N	Xenon lamp, 382 nm	2.983E+14	28740	7585	0.18
6N	Xenon lamp, 406 nm	3.78E+14	62425	13937	0.10
LC	Laser, 355 nm	1.103369E+16	970	318	0.55
1C	Laser, 355 nm	1.103369E+16	36391	5112	0.45
1C*	Xenon lamp, 355 nm	5.73E+12	36391	5112	0.45
5C	Xenon lamp, 355 nm	5.73E+12	44467	4870	0.62
6C	Xenon lamp, 367 nm	1.42E+13	110130	4950	0.43

* used as a standard for photon flux determination in a series of measurements

Table S6. Brief summary of the most important singlet excited states of **XN** and **XC** compounds as obtained from TDDFT calculations.

	Calculation		Experiment		Calculation		Experiment	
	λ , nm	f^*	λ , nm		λ , nm	f^*	λ , nm	
LN trans	453 (S_1)	0	336		LC trans	320 (S_1)	1.41	322
	331 (S_2)	1.22						
LN cis	447 (S_1)	0.05	437		LC cis	292 (S_1)	0.71	311
	280 (S_2)	0.39	263			233 (S_4)	0.29	
1N trans	353 (S_2)	1.65	365		1C trans	333 (S_1)	1.92	340
1N cis	451 (S_1)	0.08	446		1C cis	307 (S_1)	1.17	319
2N trans	352 (S_2)	1.64	364		—	—	—	—
2N cis	451 (S_1)	0.08	448		—	—	—	—
3N trans	304 (S_2)	0.78	255		—	—	—	—
3N cis	353 (S_2)	1.64	364		—	—	—	—
3N trans	451 (S_1)	0.08	448		—	—	—	—
3N cis	303 (S_2)	0.77	290		—	—	—	—
4N trans	357 (S_2)	1.59	369		—	—	—	—
4N cis	452 (S_1)	0.08	452		—	—	—	—
4N cis	308 (S_2)	0.76	340, 292, 284		—	—	—	—
5N trans	356 (S_2)	1.68	372		5C trans	335 (S_1)	1.97	341
5N cis	452 (S_1)	0.08	450		5C cis	309 (S_1)	1.24	312
6N tr-tr	308 (S_2)	0.88	283, 258		6C tr-tr	346 (S_1)	3.51	367, 351
6N cis-cis	370 (S_3)	3.11	397		6C cis-cis	319 (S_1)	1.99	318
6N cis-cis	318 (S_3)	1.47	465		6C cis-cis	305 (S_2)	0.26	
						275 (S_3)	0.01	
6N cis-tr	453 (S_1)	0.11	—		6C cis-tr	340 (S_1)	2.46	—
6N cis-tr	364 (S_3)	1.78			6C cis-tr	311 (S_2)	0.41	

* f is oscillator strength

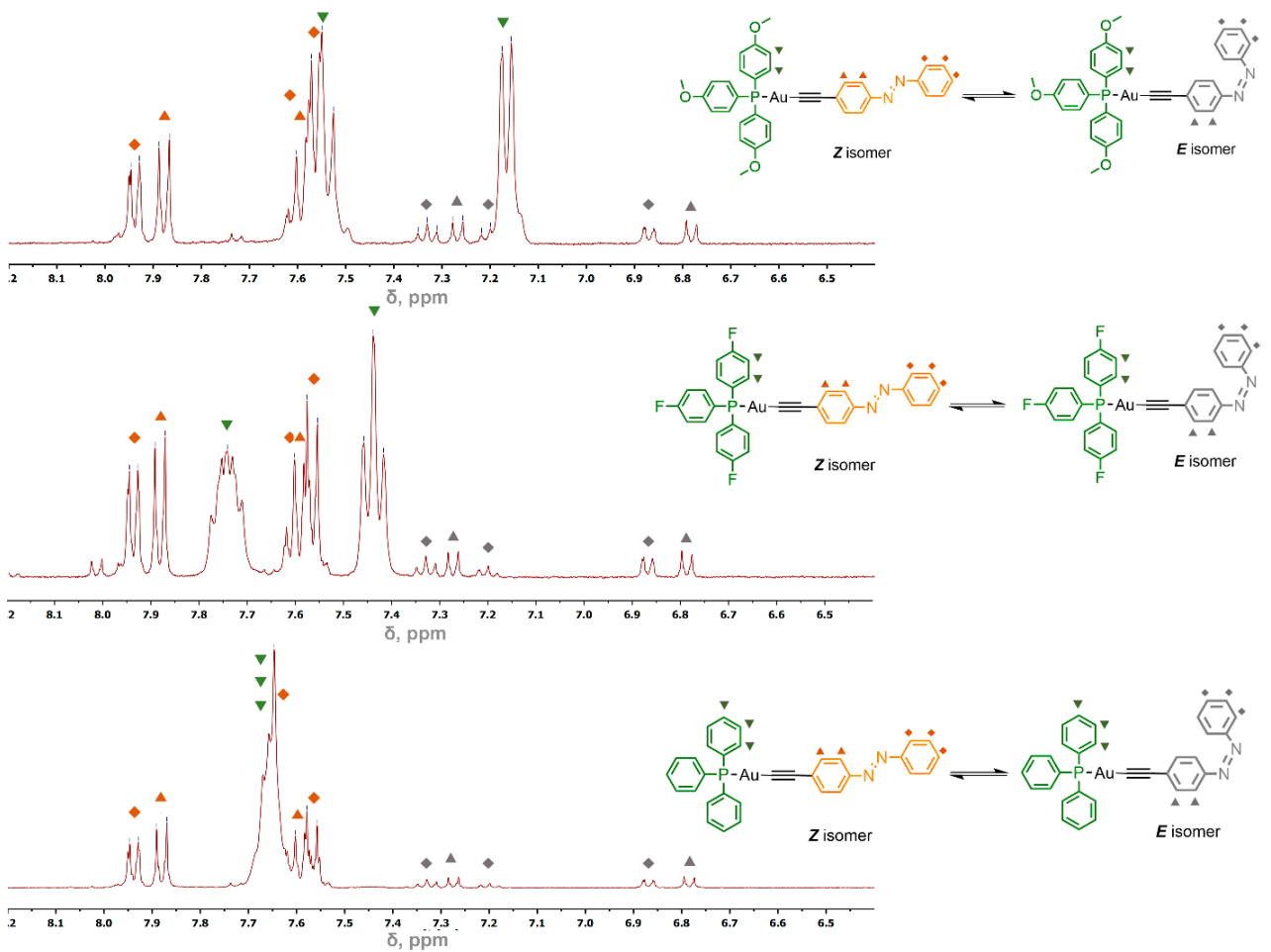


Figure S1. ^1H NMR spectra of **1N–3N**, Acetone- d_6 , r.t.

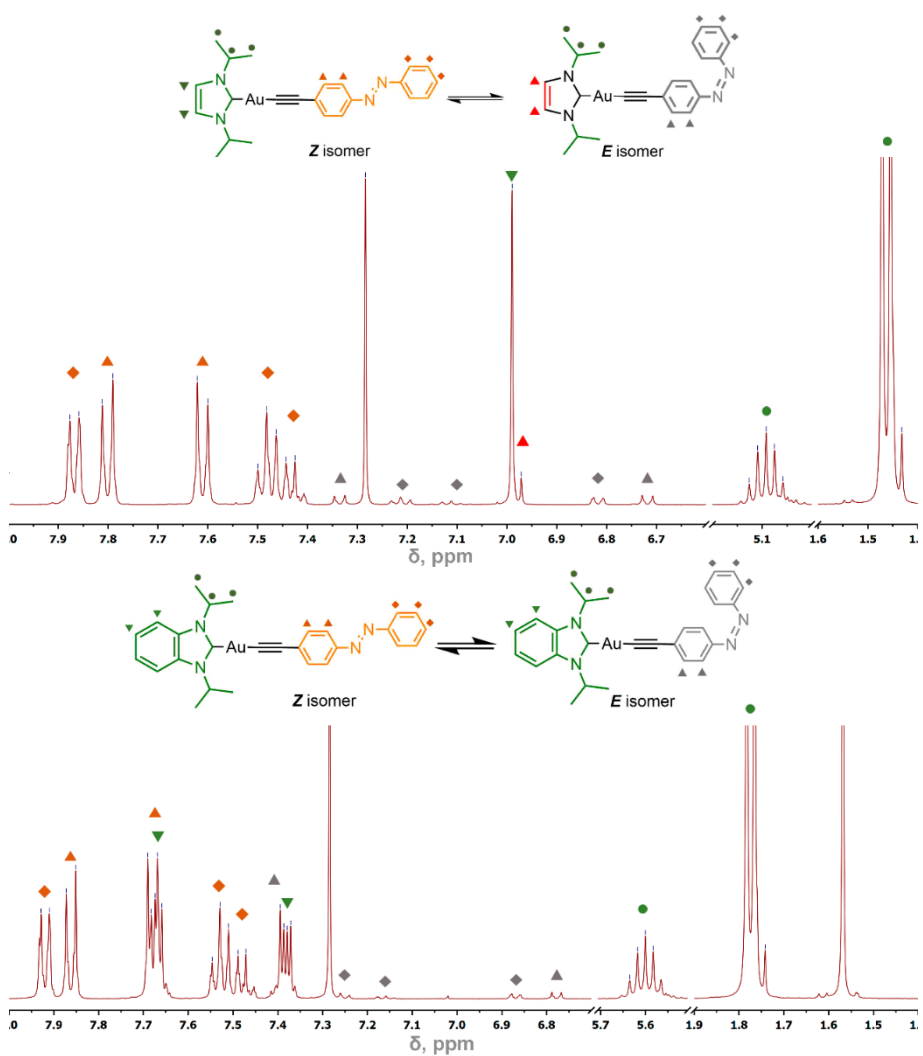


Figure S2. ^1H NMR spectra of **4N** and **5N**, Chloroform-*d*, r.t.

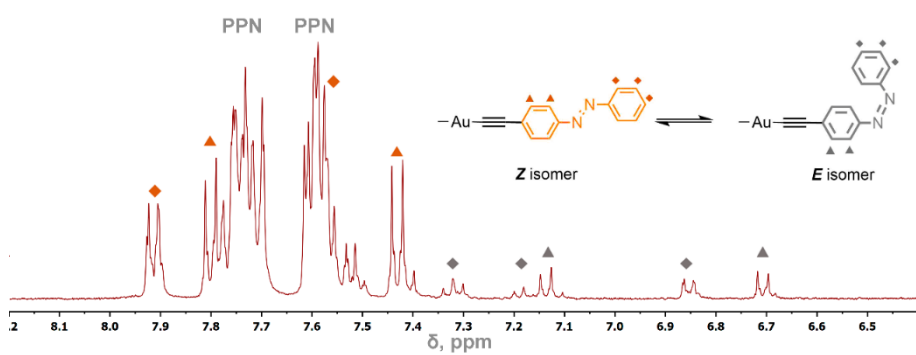


Figure S3. ^1H NMR spectrum of **6N**, Acetone-*d*₆, r.t.

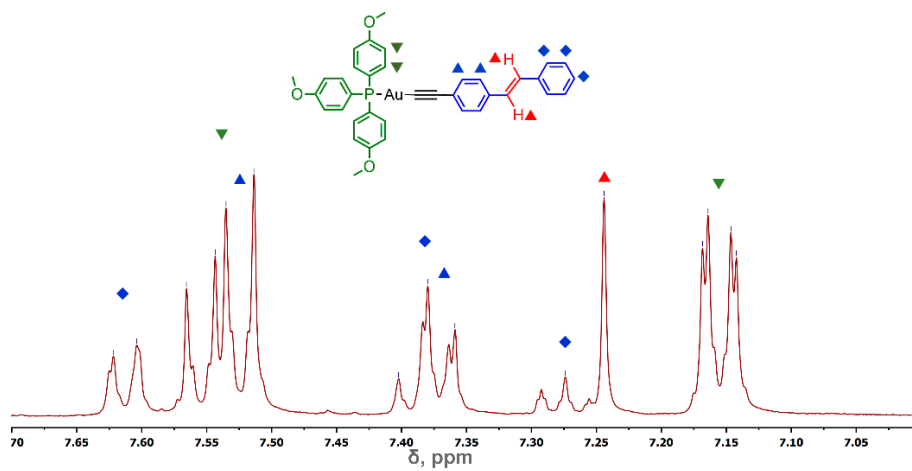


Figure S4. ¹H NMR spectrum of **1C**, Acetone-*d*₆, r.t.

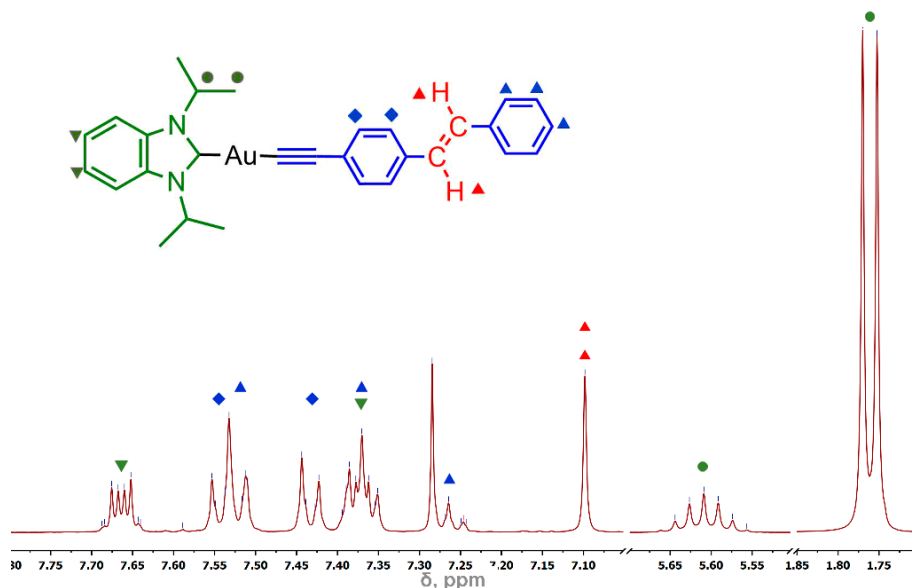


Figure S5. ¹H NMR spectrum of **5C**, Chloroform-*d*, r.t.

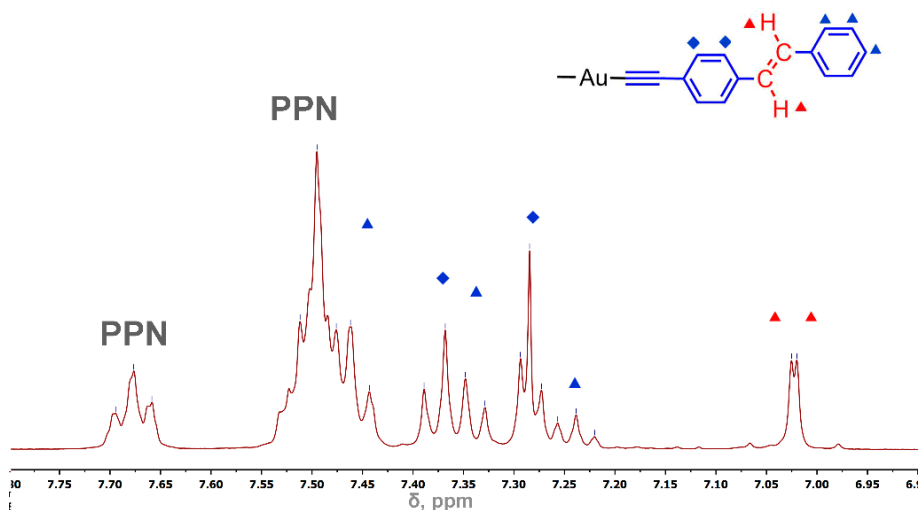


Figure S6. ^1H NMR spectrum of **6C**, Chloroform-*d*, r.t.

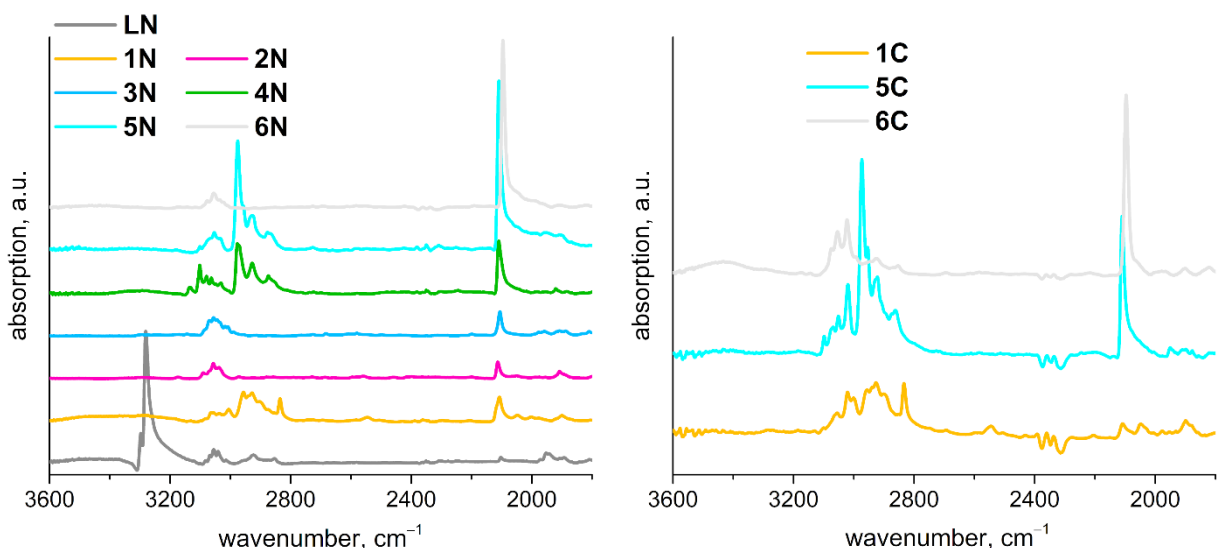


Figure S7. FTIR spectra of azobenzene and stilbene derivatives, KBr pellet, r.t.

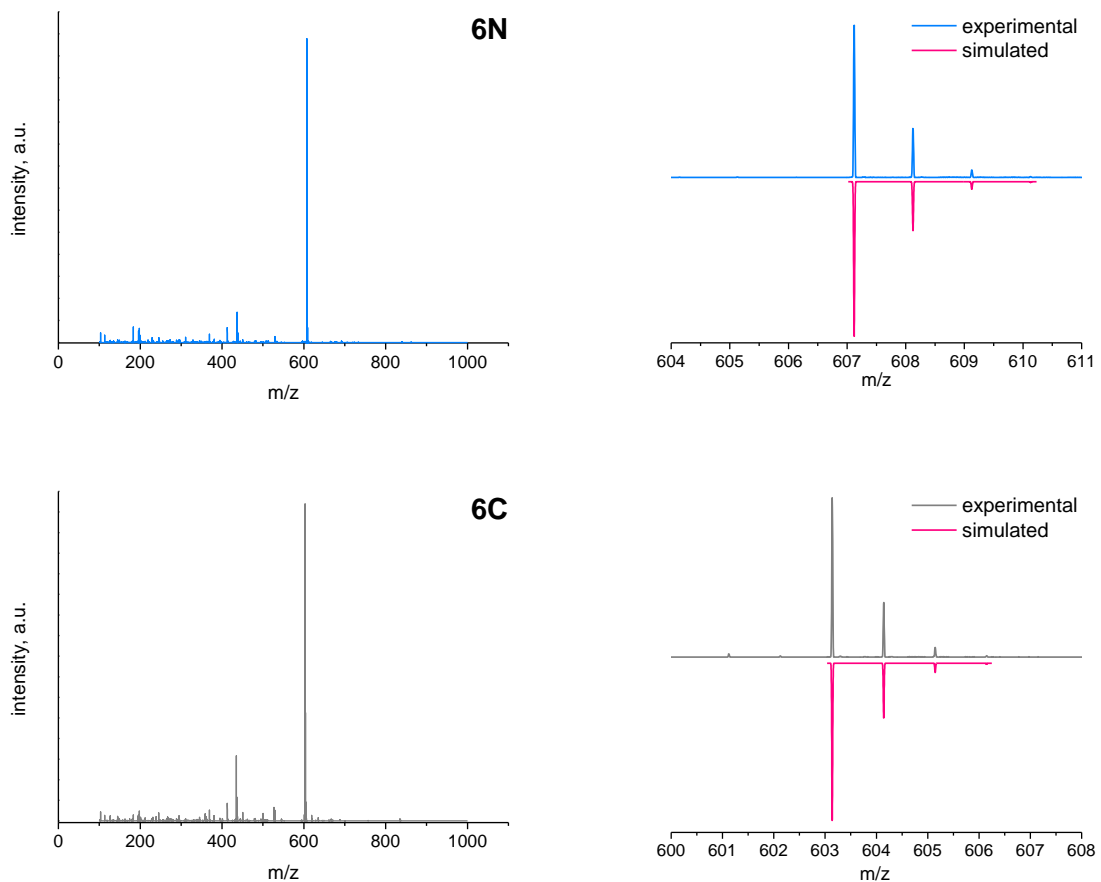


Figure S8. Experimental ESI⁻ MS spectra of **6N** and **6C**, and simulated isotopic patterns of the most intensive signal corresponded to molecular ion.

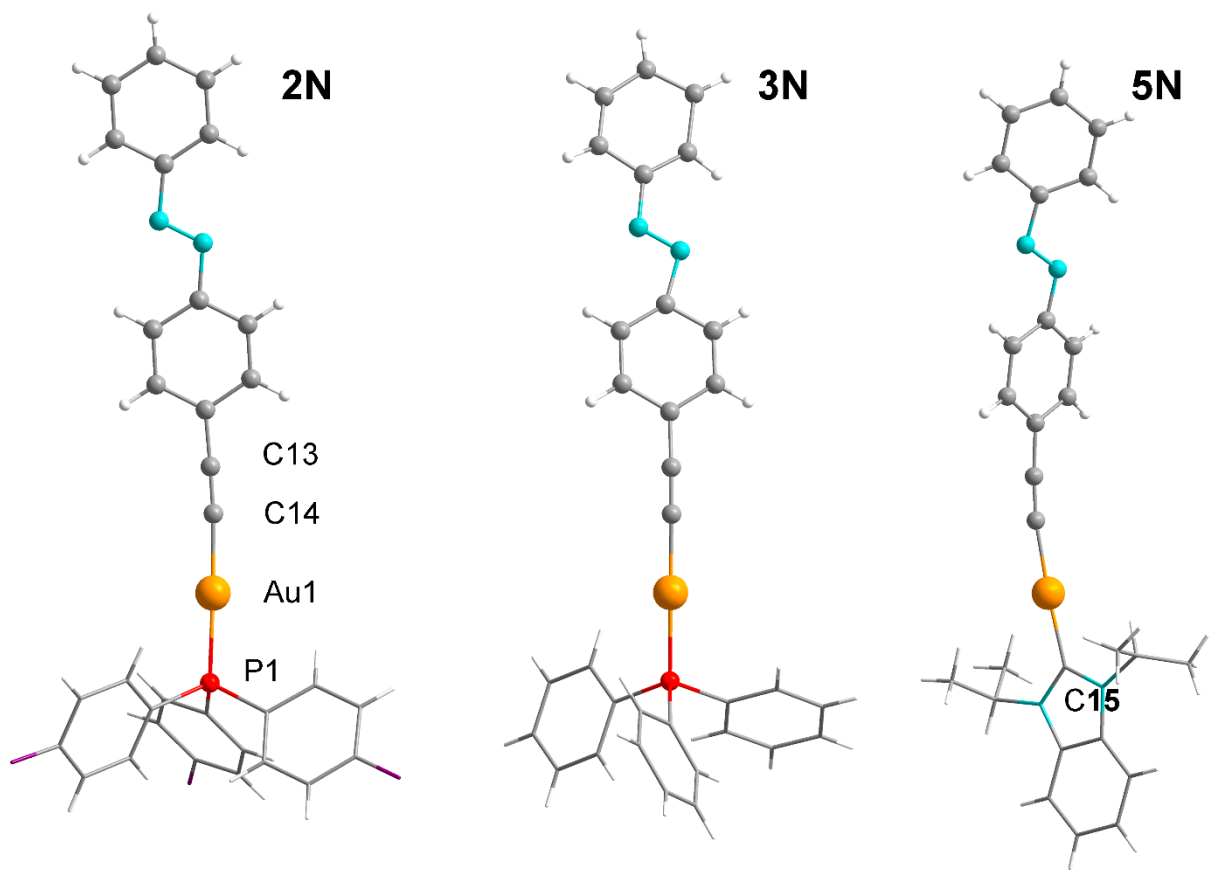


Figure S9. Molecular structure of **2N**, **3N** and **5N**.

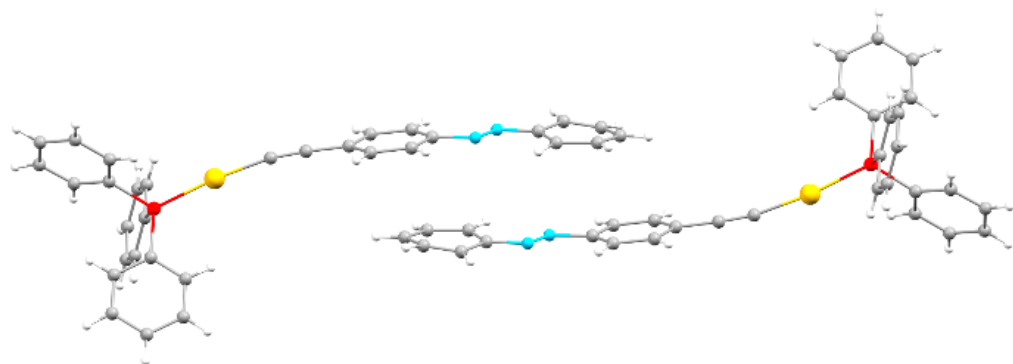


Figure S10. Mutual orientation of two molecules in the crystal packing of **3N**.

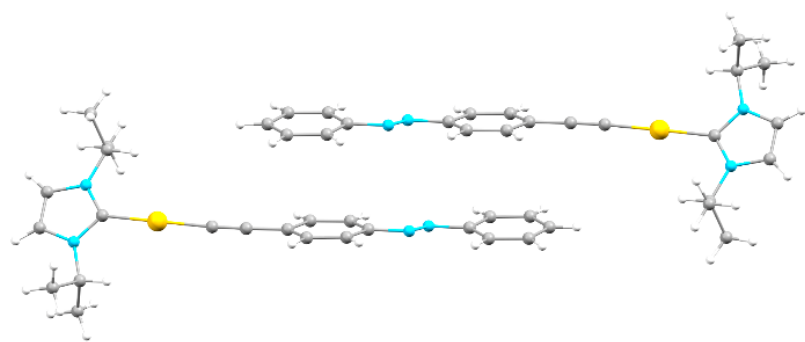


Figure S11. Mutual orientation of two molecules in the crystal packing of **4N**.

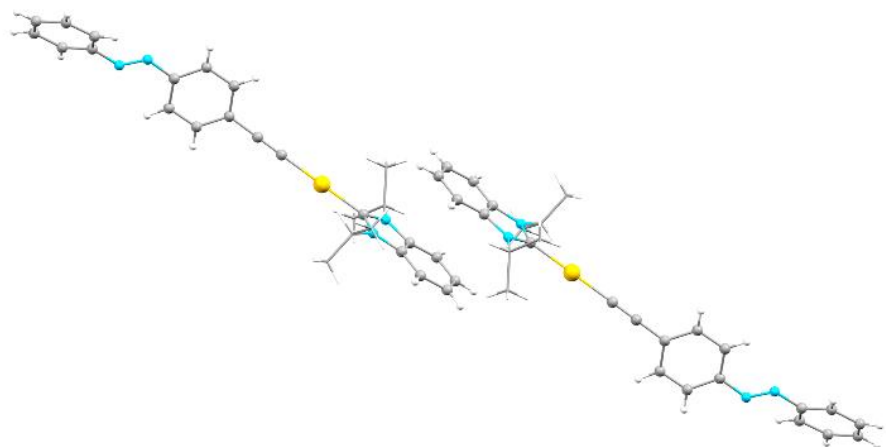


Figure S12. Mutual orientation of two molecules in the crystal packing of **5N**.

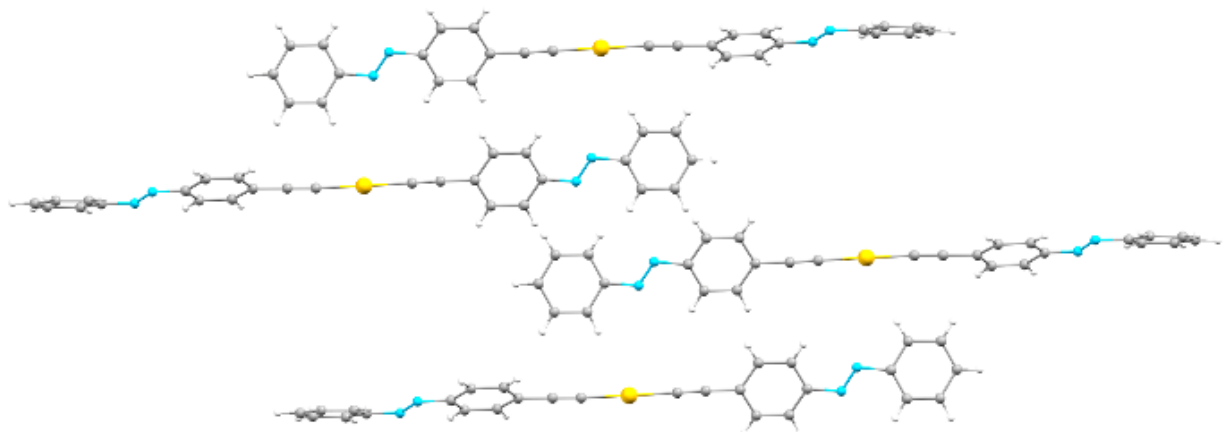


Figure S13. Mutual orientation of molecules in the crystal packing of **6N**.

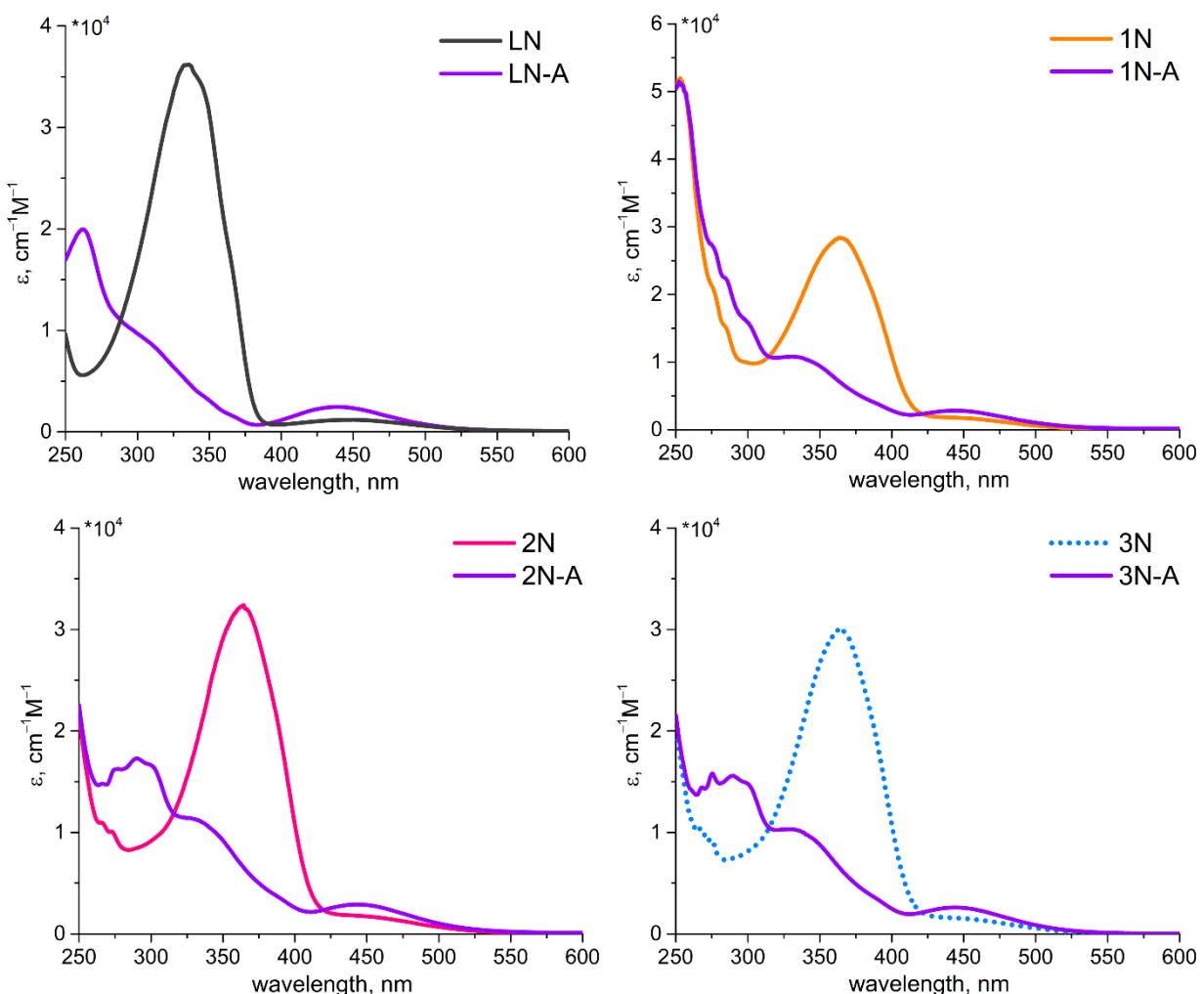


Figure S14. UV-vis spectra of **LN** and Au(I) complexes **XN** ($X = 1\text{--}3$) before and after (line marked by ‘A’) UV irradiation, DCE, r.t. In the cases of irradiated samples formal ϵ values based on total concentrations are calculated.

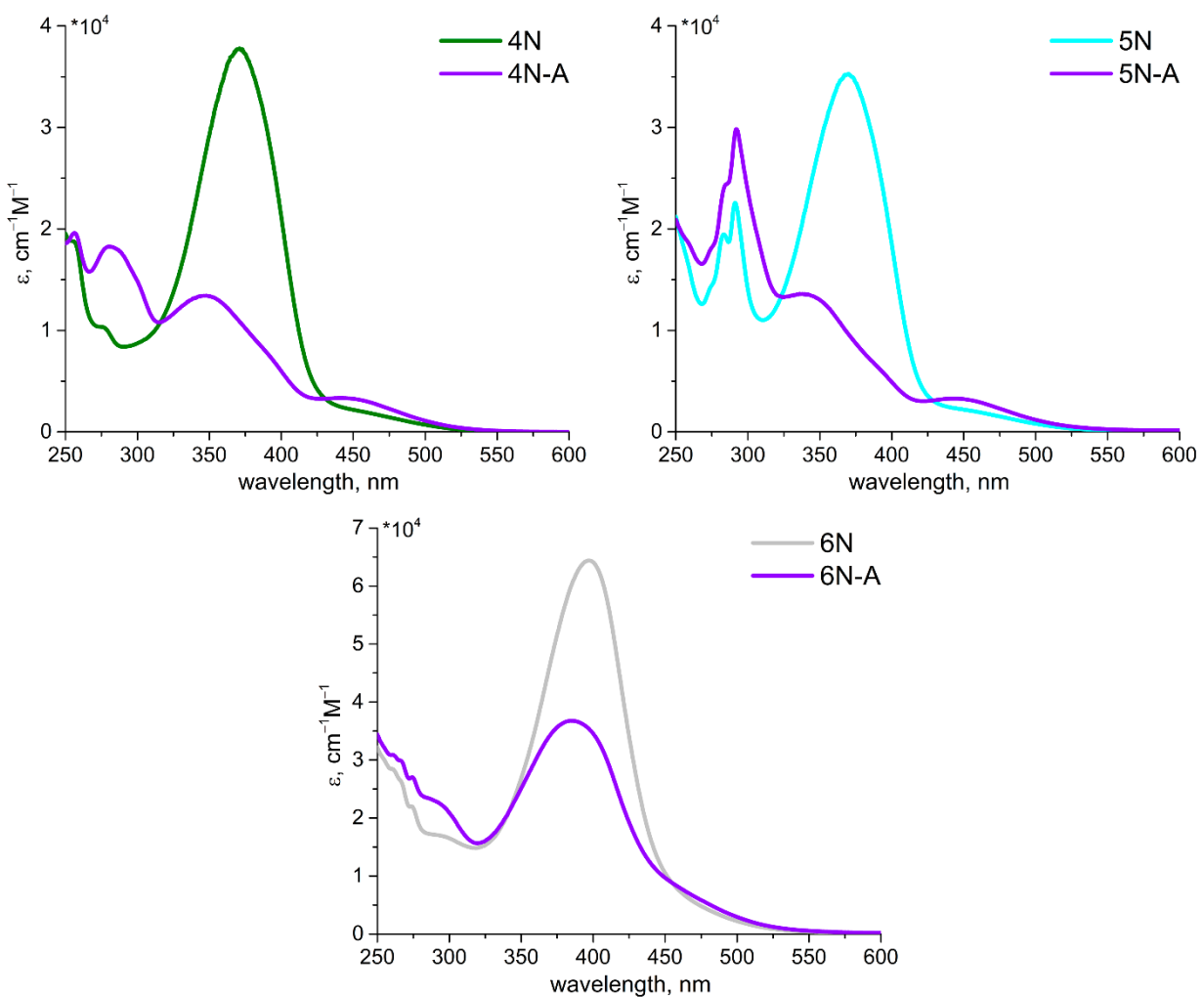


Figure S15. UV-vis spectra of Au(I) complexes **XN** ($X = 4–6$) before and after (line marked by ‘A’) UV irradiation, DCE, r.t. In the cases of irradiated samples formal ϵ values based on total concentrations are calculated.

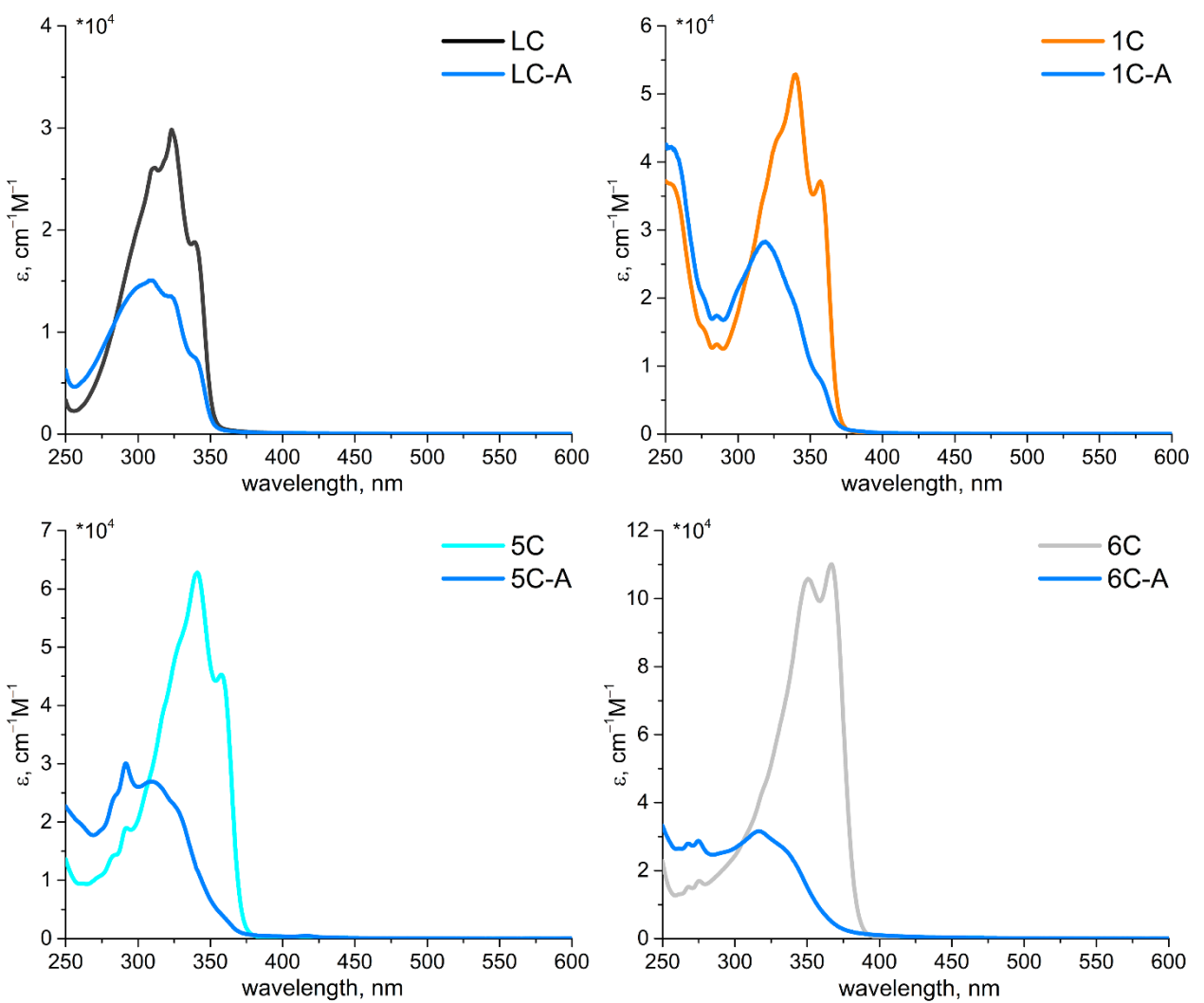
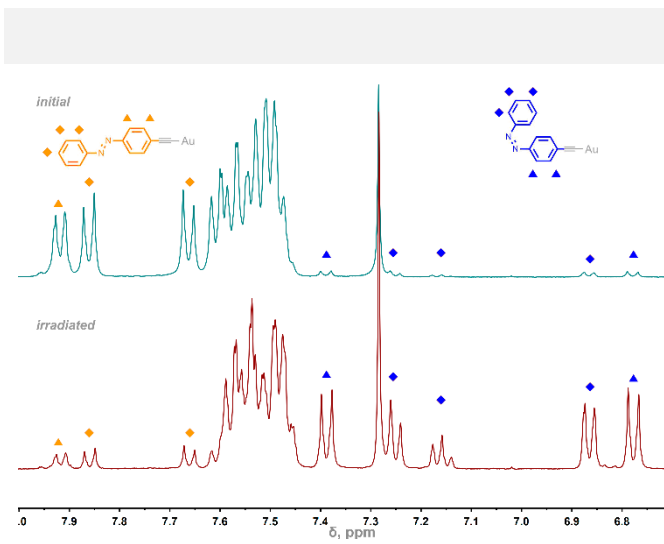
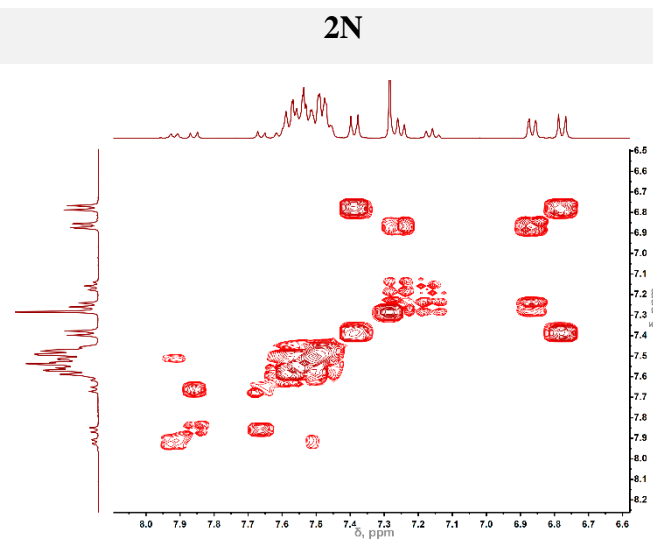


Figure S16. UV-vis spectra of **LC** and Au(I) complexes **XC** ($X = 1, 5, 6$) before and after (line marked by ‘A’) UV irradiation, DCE, r.t. In the cases of irradiated samples formal ϵ values based on total concentrations are calculated.

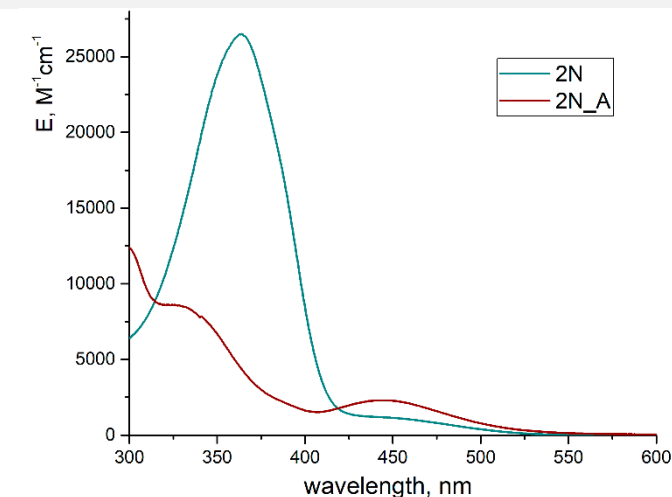
^1H NMR spectrum before (green line)
and after (red line) UV irradiation



$^1\text{H}^1\text{H}$ COSY NMR spectrum after UV irradiation



UV-Vis spectrum before (green line)
and after (red line) UV irradiation



5N

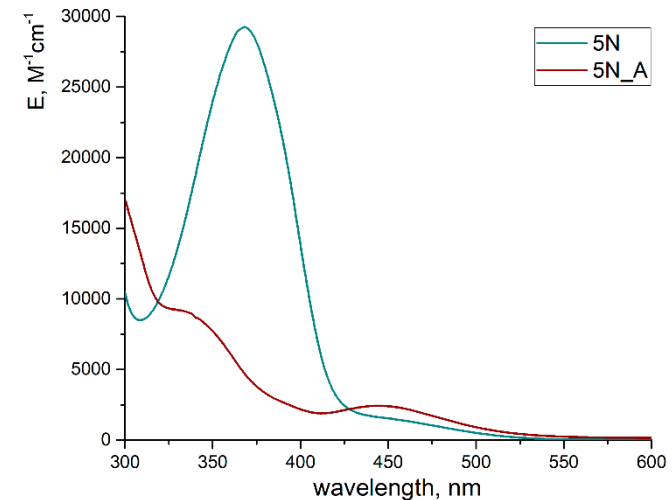
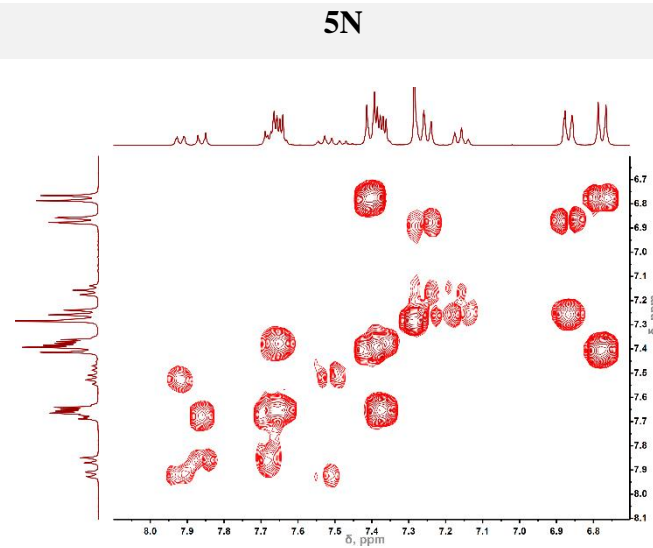
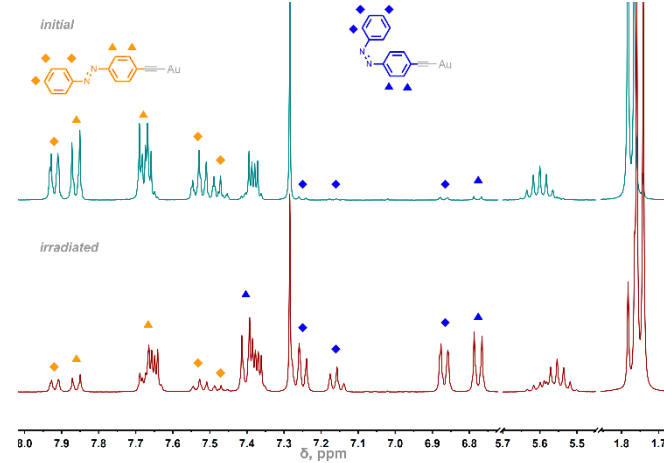
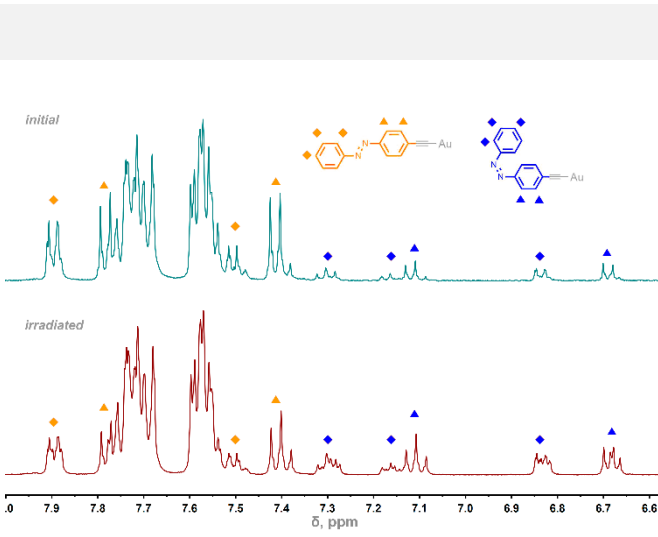
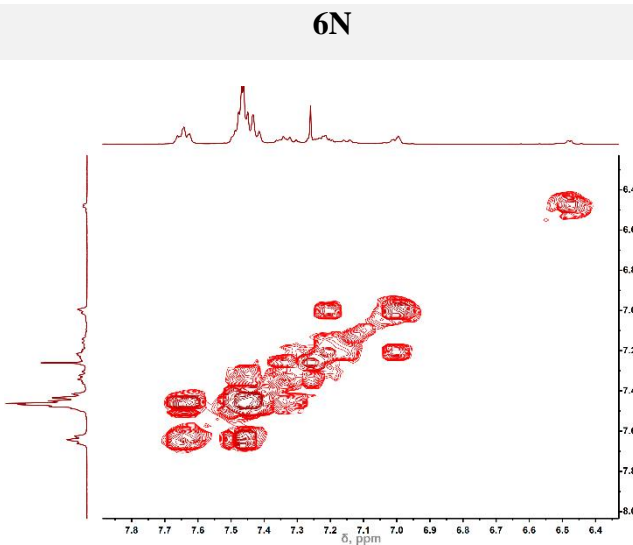


Figure S17. ^1H and $^1\text{H}^1\text{H}$ COSY NMR, and UV-Vis spectroscopic monitoring of representative complexes **XN** and **XC** photoisomerization.

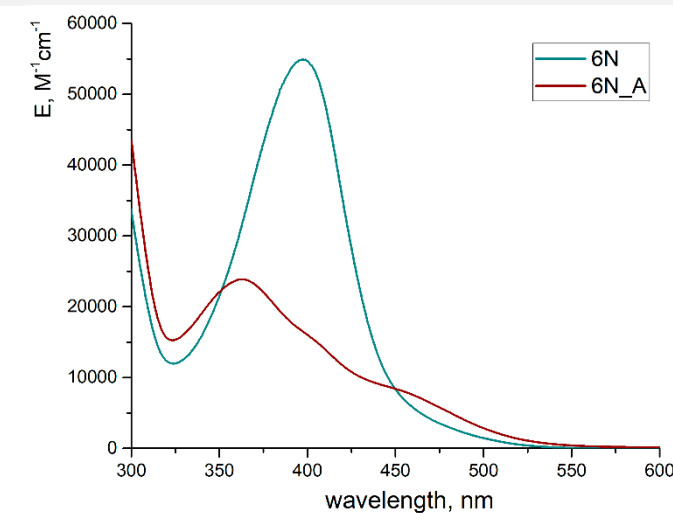
^1H NMR spectrum before (green line)
and after (red line) UV irradiation



$^1\text{H}^1\text{H}$ COSY NMR spectrum after UV irradiation



UV-Vis spectrum before (green line)
and after (red line) UV irradiation



1C

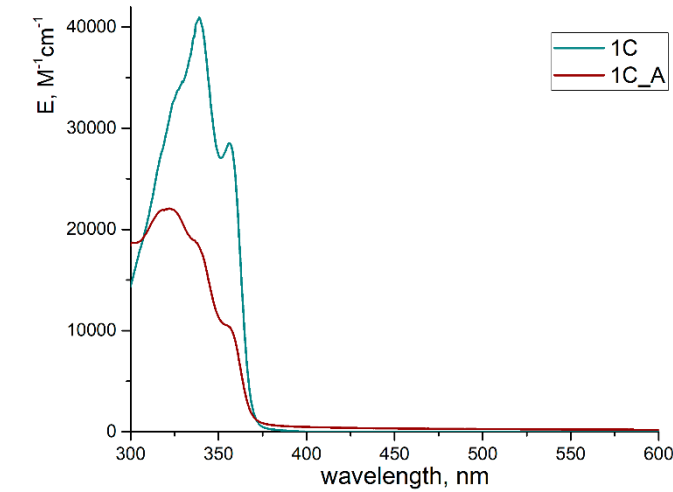
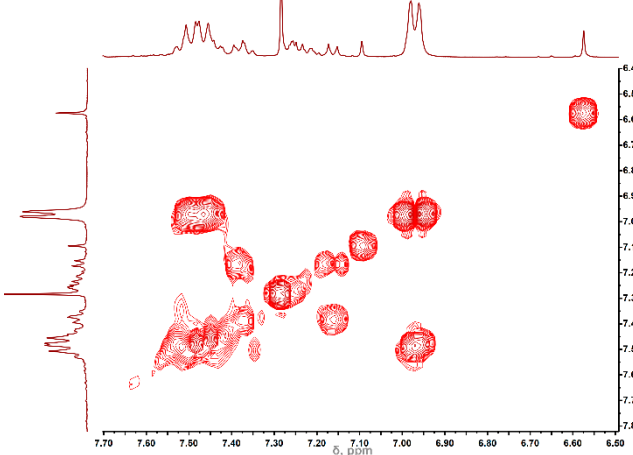
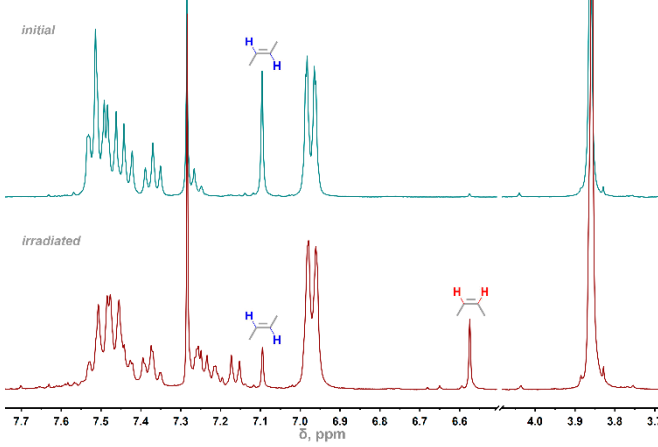
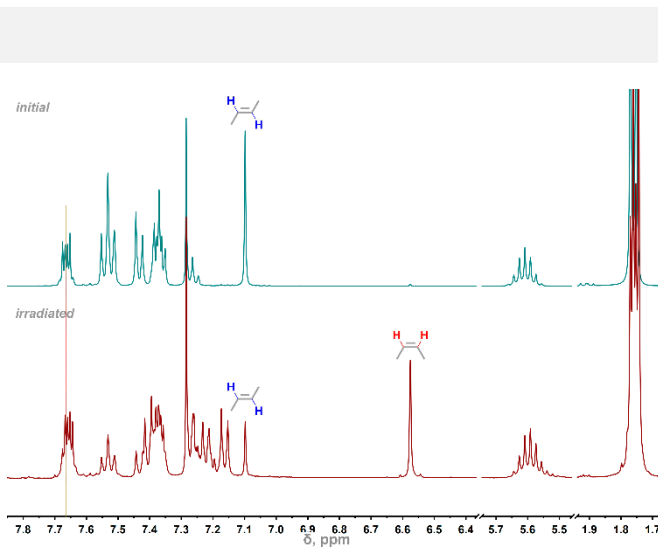
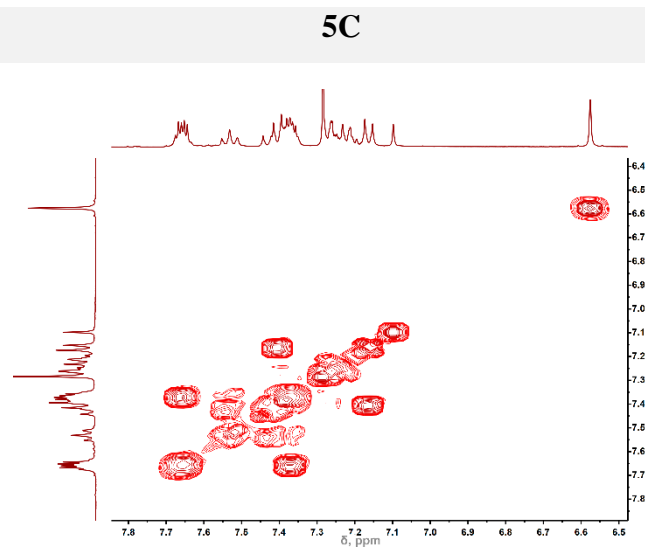


Figure S17 Continued.

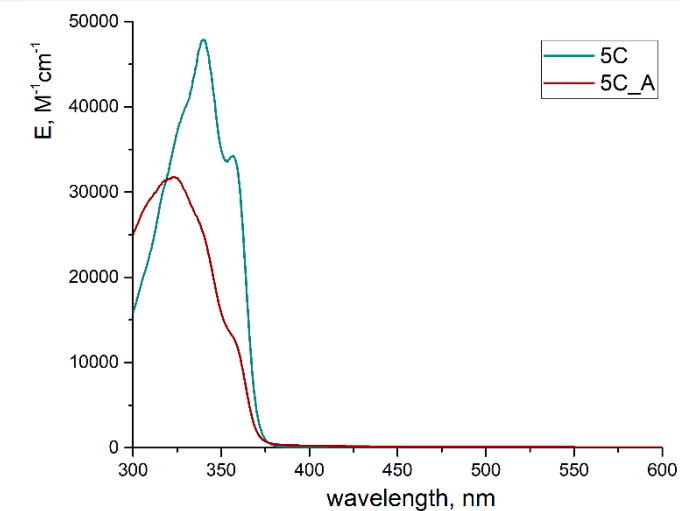
^1H NMR spectrum before (green line)
and after (red line) UV irradiation



$^1\text{H}^1\text{H}$ COSY NMR spectrum after UV irradiation



UV-Vis spectrum before (green line)
and after (red line) UV irradiation



6C

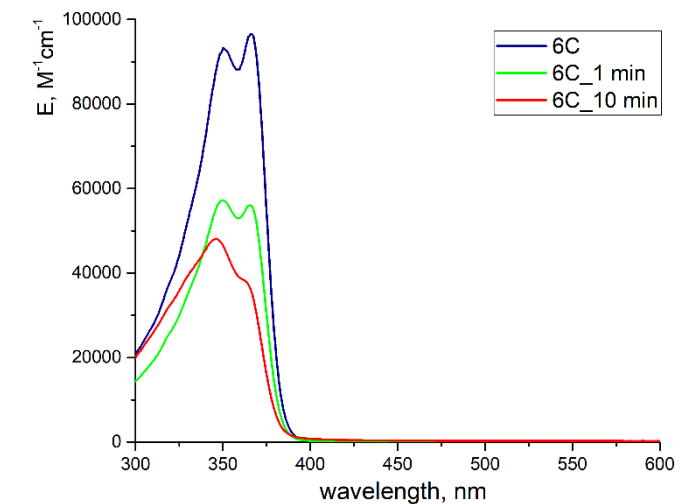
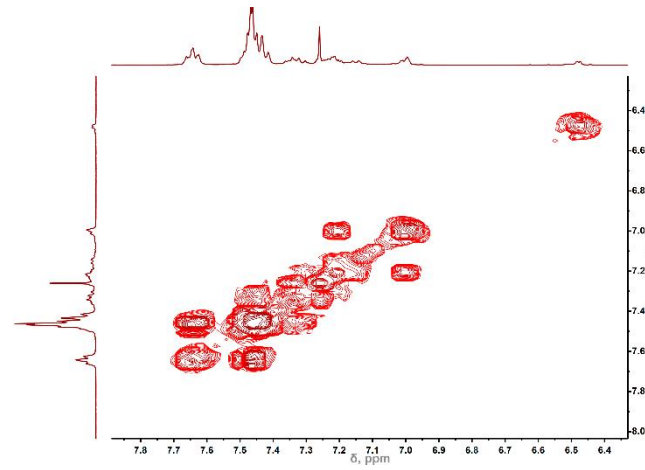
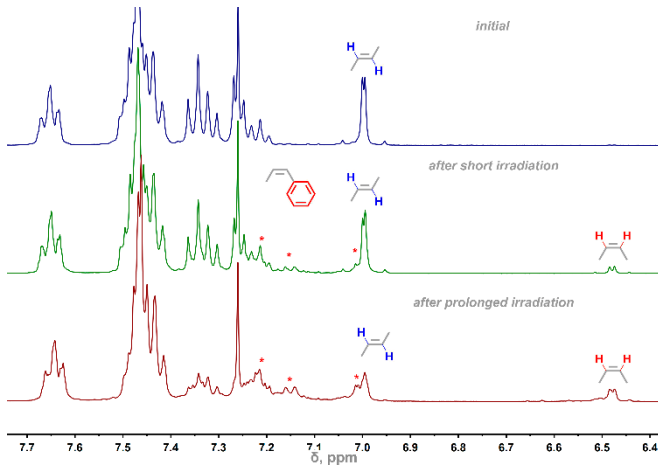


Figure S17 Continued.

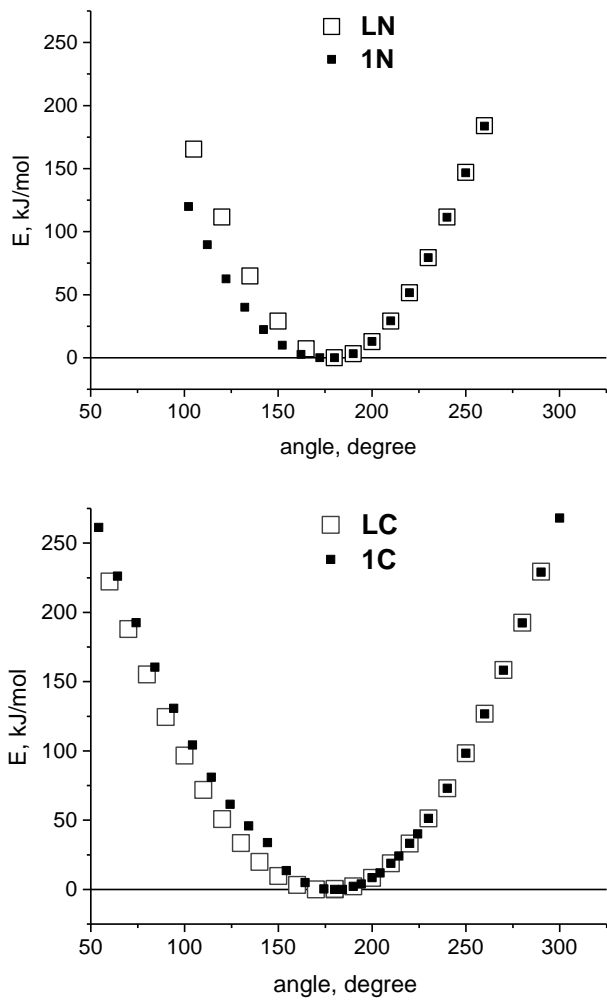


Figure S18. Dihedral energy scans corresponding to rotation around N=N and C=C bonds:
DFT computational data.

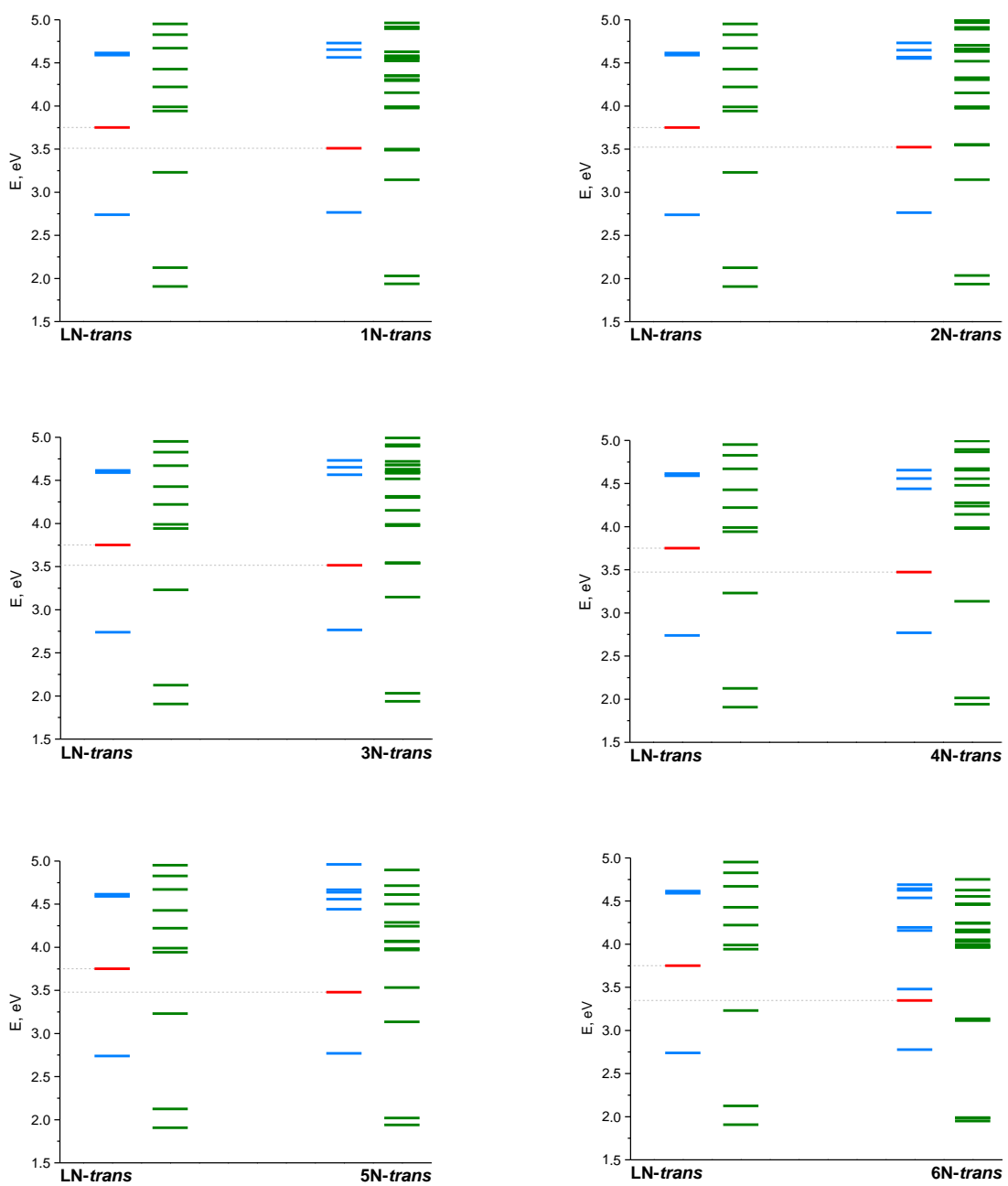


Figure S19. Energy level diagram of the excited states in XN obtained from TDDFT calculations. Colour legend shows singlets (blue), triplets (green), and low-lying active states (red).

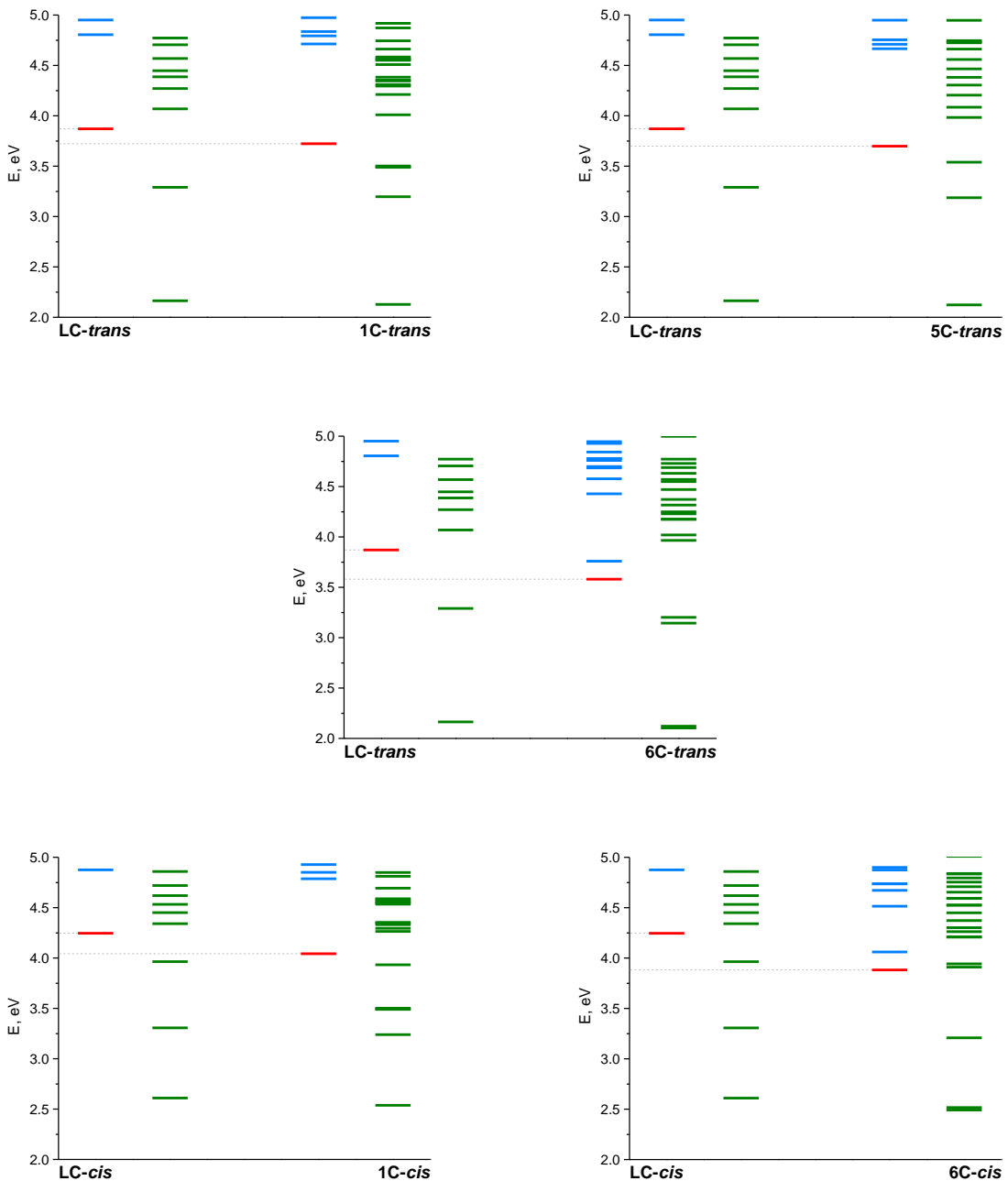


Figure S20. Energy level diagram of the excited states in XC obtained from TDDFT calculations. Colour legend shows singlets (blue), triplets (green), and low-lying active states (red).

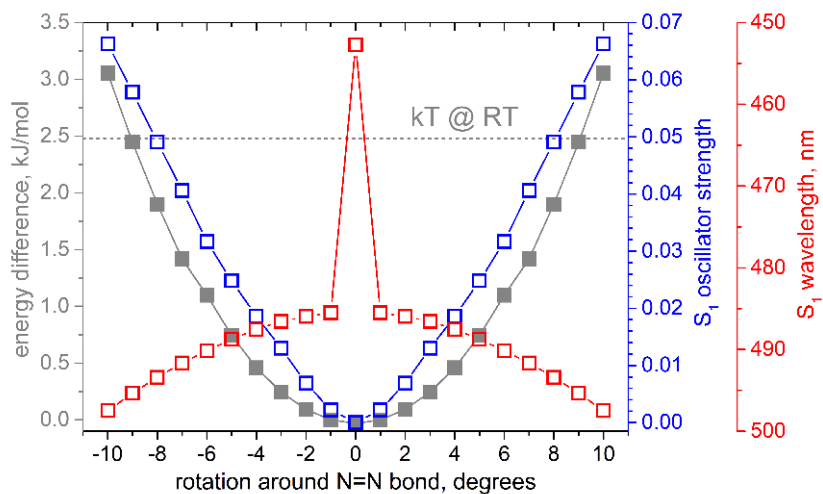


Figure S21. Evolution of the S_1 state in LN upon low-angle rotation around the N=N bond. Wavelengths and oscillator strengths are obtained from TDDFT calculations. Ground state energy curve is shown to demonstrate the relatively high probabilities of such rotations via comparison with kT value at room temperature.

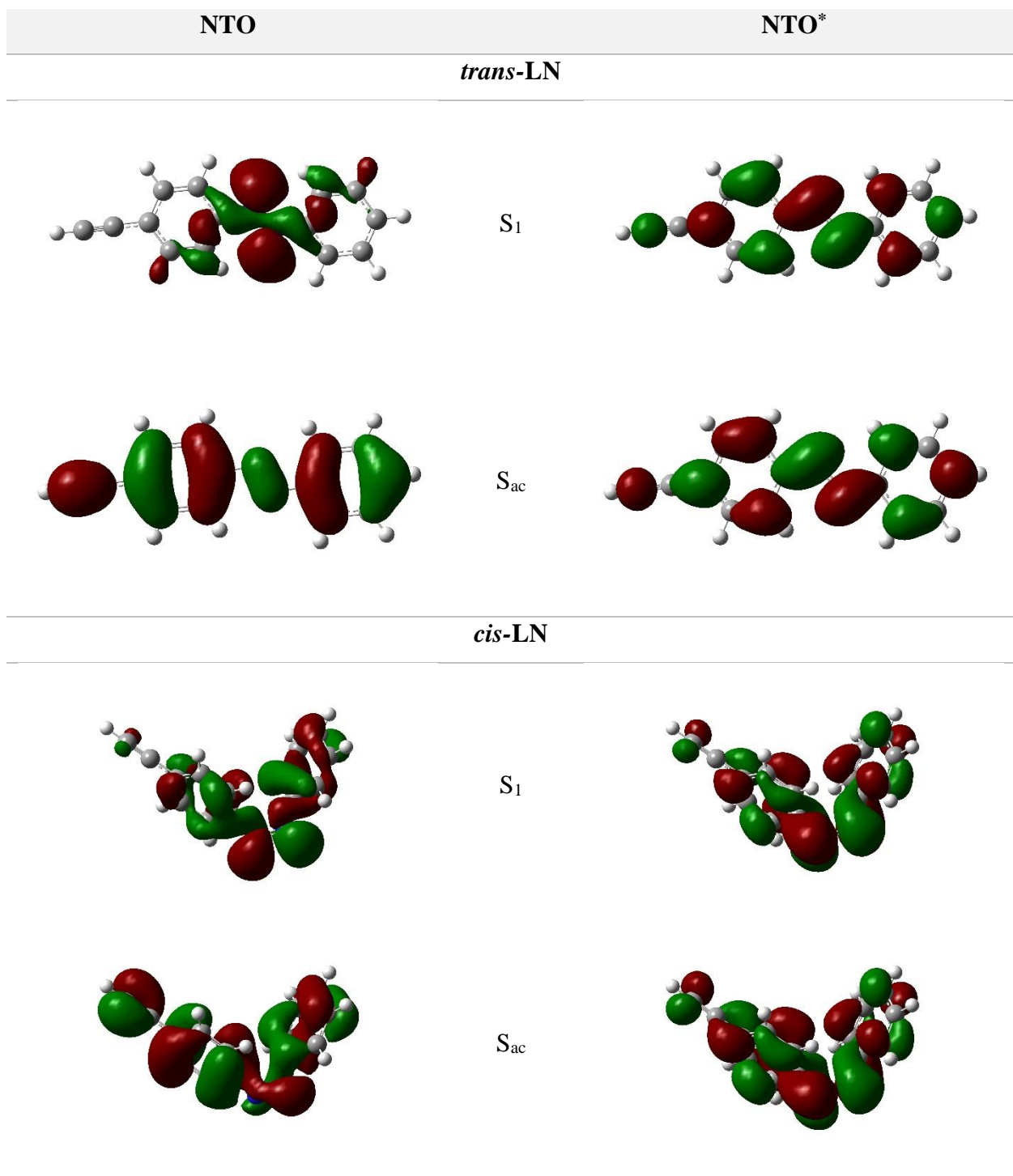


Figure S22. Natural transition orbitals involved in the lowest energy electronic excitation for compound **LN**.

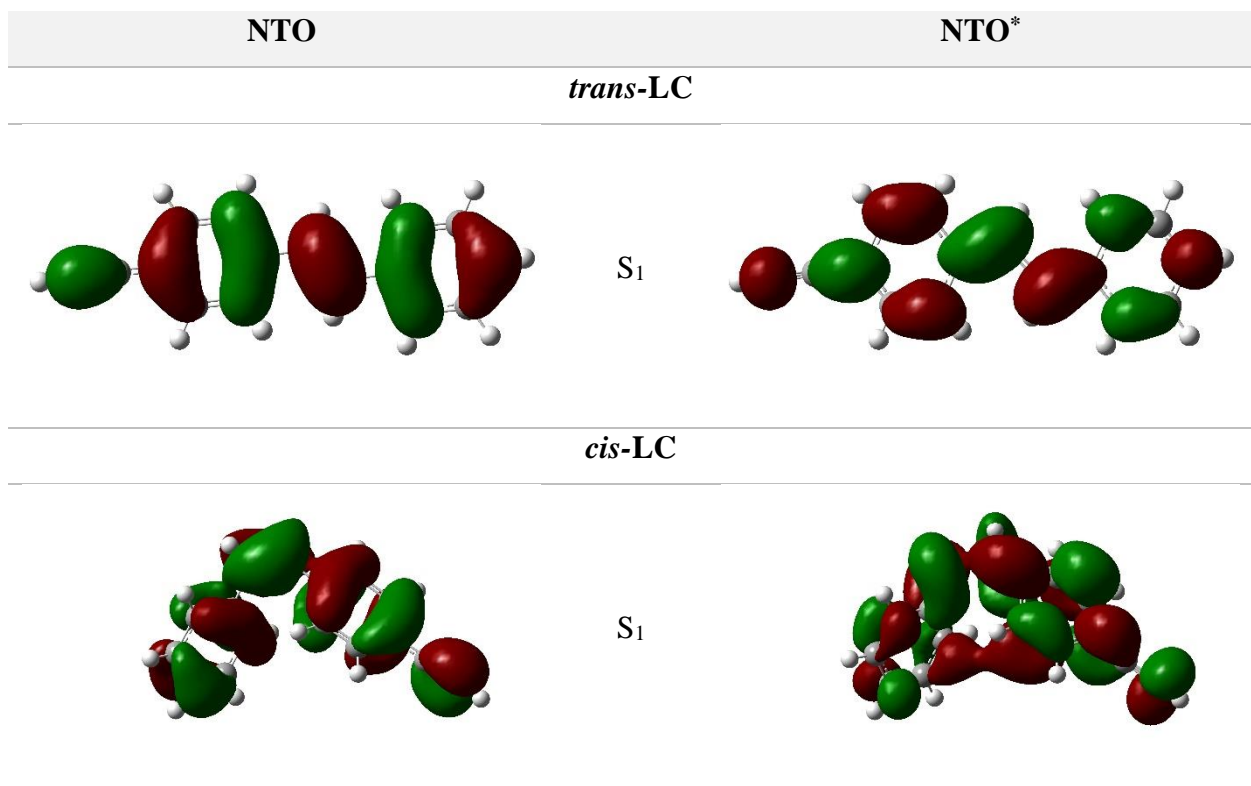
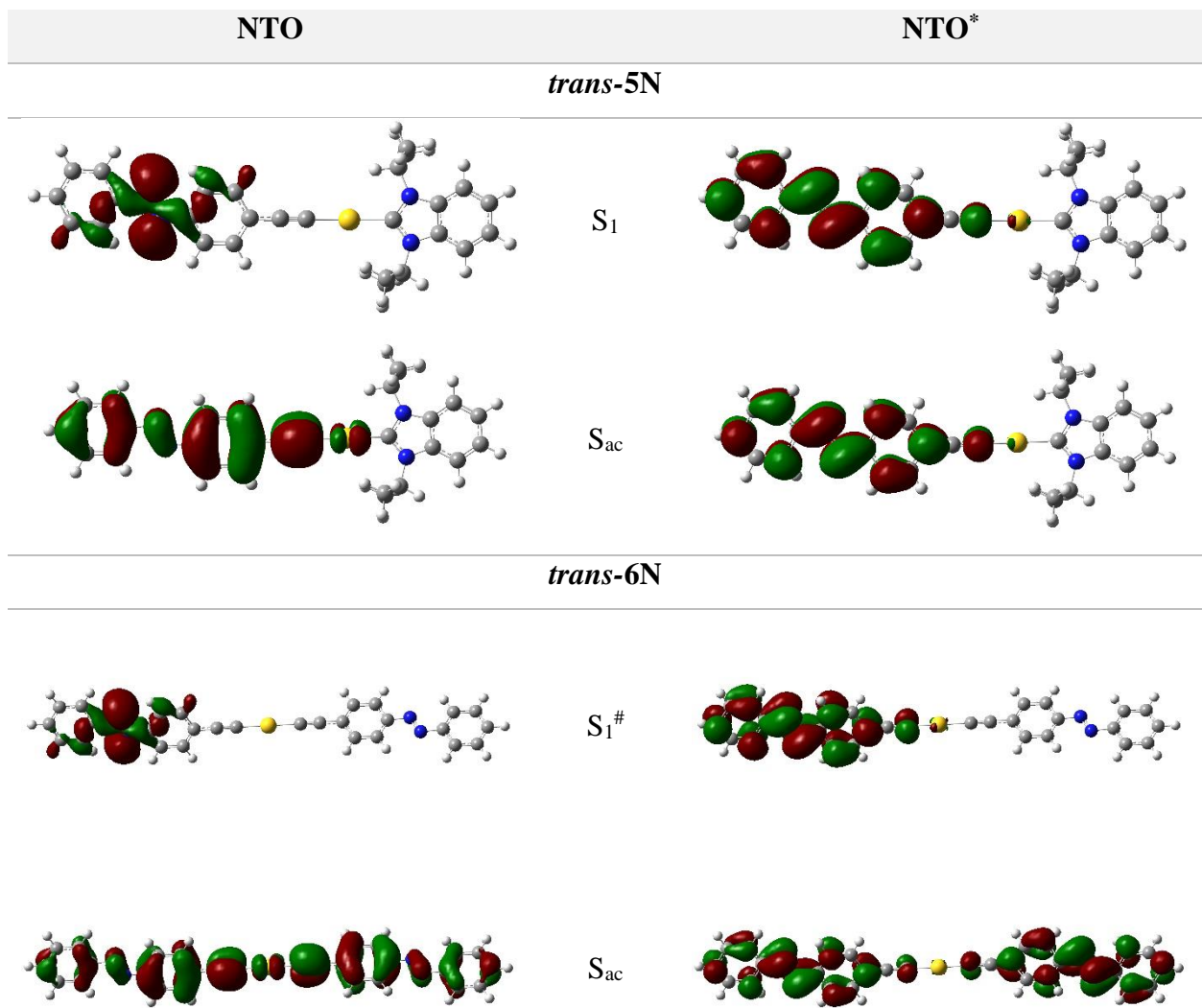


Figure S23. Natural transition orbitals involved in the lowest energy electronic excitation for compound **LC**.



[#] For **trans**-**6N** two degenerate intraligand singlet states are observed in TDDFT calculations, with each of the states being localized on one of the ligands. Only one of these states is shown for clarity.

Figure S24. Natural transition orbitals involved in the lowest energy electronic excitation for compounds **5N** and **6N** in *trans*-form of switcher group.

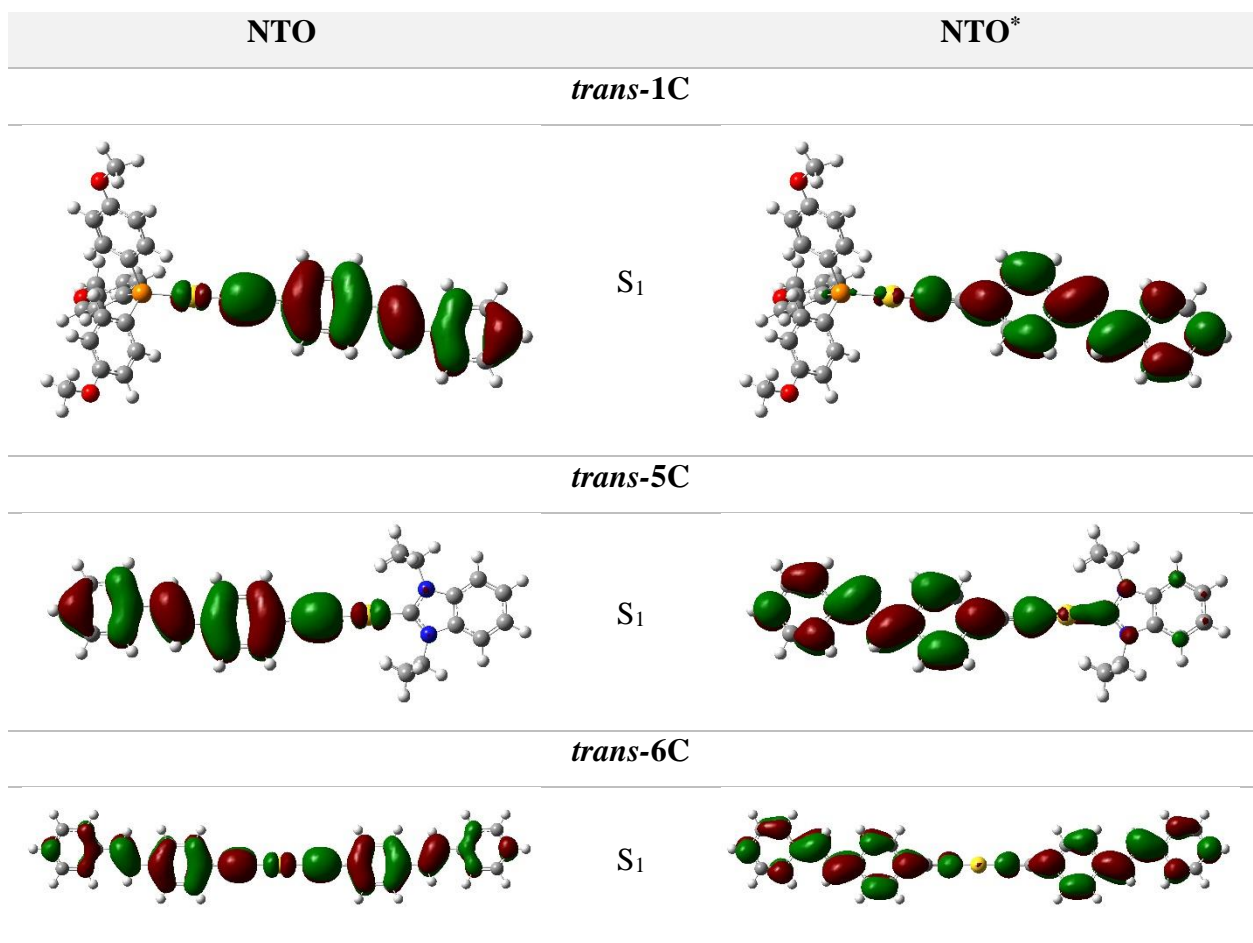


Figure S25. Natural transition orbitals involved in the lowest energy electronic excitation for compounds XC ($X = 1, 5, 6$) in *trans*-form of switcher group.

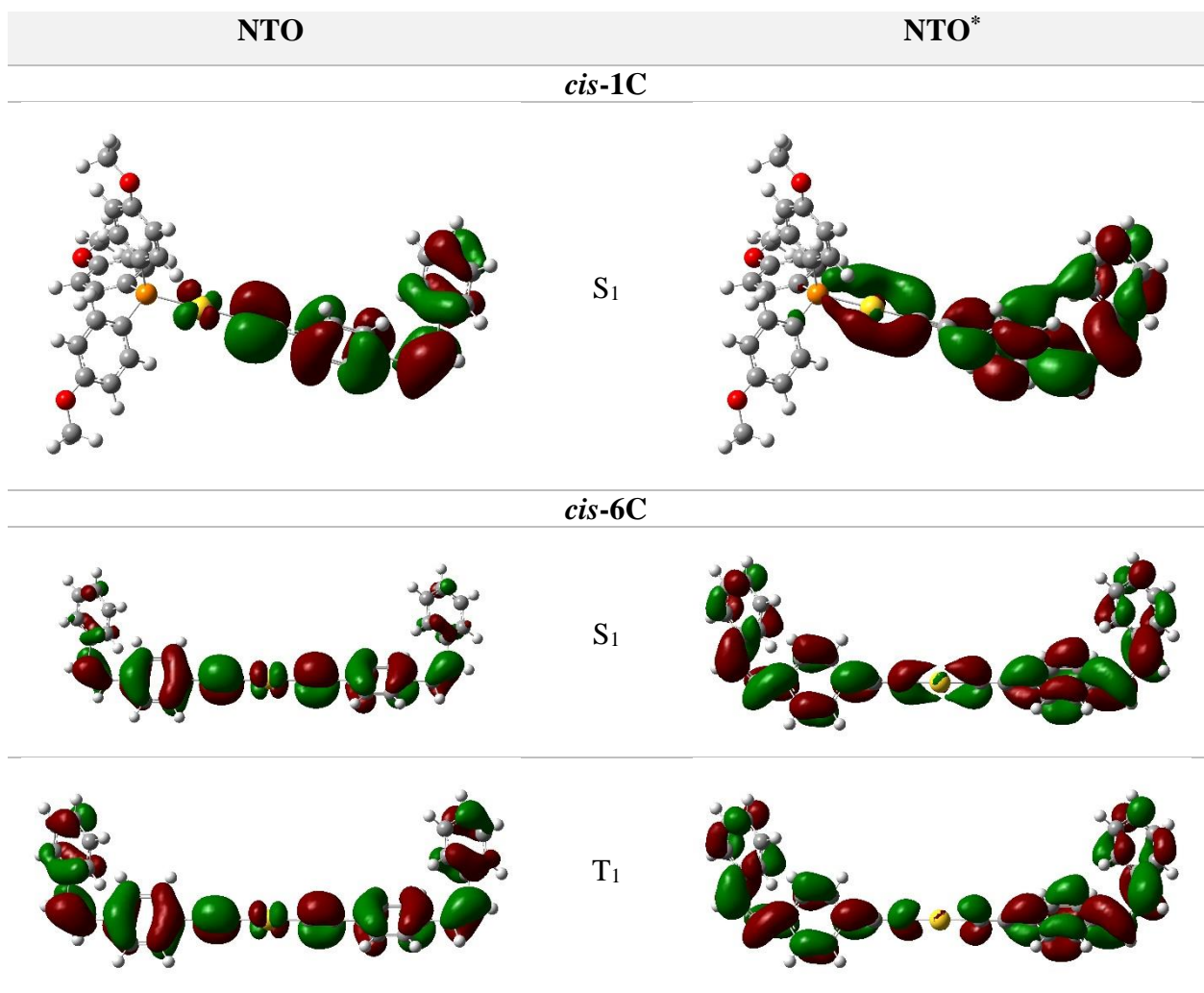


Figure S26. Natural transition orbitals involved in the lowest energy electronic excitation for compounds **1C** and **6C** in *cis*-form of switcher group.

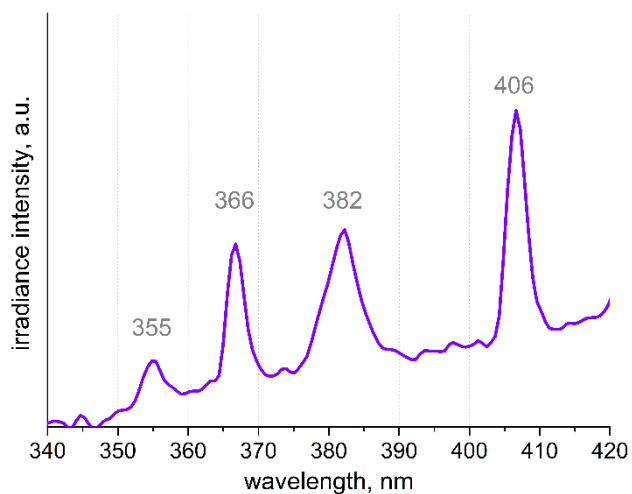


Figure S27. Emission spectrum of xenon lamp in soft UV region.

References

- 1 *CrysAlisPro, Rigaku Oxford Diffraction*, Agilent Technologies, Version 1.171.39.35a, 2017.
- 2 G. M. Sheldrick, *Acta Crystallogr. Sect. A Found. Adv.*, 2015, **71**, 3–8.
- 3 G. M. Sheldrick, *Acta Crystallogr. Sect. C*, 2015, **71**, 3–8.
- 4 O. V. Dolomanov, L. J. Bourhis, R. J. Gildea, J. A. K. Howard and H. Puschmann, *J. Appl. Crystallogr.*, 2009, **42**, 339–341.